process, reduced zygomatic arch, long narrow muzzle, broad supraorbital process, and teeth that resemble those of other archaeocetes, the paraphyletic stem group of cetaceans. Archaic archaeocete whales have been found in Africa (*16, 17*) and North America (*18, 19*), but are best known from Pakistan and India (*2, 20–22*), and it is likely that cetaceans originated near the subcontinent. Thus, the skeletal morphology of *Ambulocetus* is critical to our understanding of locomotion in early cetaceans.

The closest terrestrial relatives of whales, mesonychids, were running mammals (*10, 23*) that, when swimming, probably paddled by flexing and extending their hindlimbs alternately as in extant land mammals (*24*). At some point, cetaceans switched from unilateral paddling to bilateral (spinal) undulating (*25*) and from using the feet as a primary propulsive surface to having a tail fluke. *Ambulocetus* shows that spinal undulation evolved before the tail fluke. These fossils also test several hypotheses concerning early whale locomotion. The greatly expanded feet imply that forelimb propulsion is not primitive for cetaceans even though it may occur in other protocetids (*12*). It corroborates that cetaceans have gone through a stage that combined hindlimb paddling and spinal undulation, resembling the aquatic locomotion of fast swimming otters (*25, 26*). Unlike modern cetaceans, *Ambulocetus* certainly was able to walk on land, probably in a way similar to modern sea lions or fur seals. In water, it combined aspects of the locomotion of modern seals, otters, and cetaceans: Like modern cetaceans it swam by moving its spine up and down, but like seals, the main propulsive surface was provided by its feet. As such, *Ambulocetus* represents a critical intermediate between land mammals and marine cetaceans.

REFERENCES AND NOTES

1. R. M. West, *J. Paleontol.* **54**, 508 (1980).
2. J. G. M. Thewissen and S. T. Hussain, *Nature* **361**, 444 (1993).
3. Order Cetacea, Suborder Archaeoceti, Family Protocetidae.

   Ambulocetus natans, n. gen., n. sp.

   Holotype. Howard Geological Survey of Pakistan 18507: skull with left P4/-M1-2/ and lacking the rostrum, but preserving both tympanics, basihyoid, right posterior mandible with P/4, M/2-3, and left ramus with alveoli for C/1-P/3, half atlas, fragments of three other cervical vertebrae, two complete and several fragmentary thoracic and one lumbar vertebra, three complete ribs, and a sternebra. Forelimb fragments include part of the glenoid, left and right radius and ulna, all left carpals except the triquetrum, all metacarpals, and at least four proximal, two intermediate phalanges, and a fragment of one distal phalanx. Hindlimb elements include complete femur, proximal tibia, distal fibula, trochlea of astragalus, metatarsals II–V and at least two proximal, three intermediate, and three distal phalanges. The holotype was found at locality HGSP 9209 in the upper Kuldana Formation, Punjab, 3.7 km northwest of Ganda Kas (72°12′20″E, 33°39′N). *Referred material.* P/2 (HGSP 18473), P/3 (HGSP 18497), caudal vertebra (HGSP 18472), and distal femur (HGSP 18476), all from locality 9207, about 5 m above the type locality in the section. All material will be housed at the Geological Survey of Pakistan in Islamabad. *Known distribution.* Kala Chitta Hills of Pakistan, upper Kuldana Formation and transitional beds to the Kohat Formation. Lower to middle Eocene. *Differential diagnosis of genus.* P4/ of *Ambulocetus* has a single high labial cusp, unlike *Protocetus* (*16*), but lacks a protocone. M1/ and M2/ of *Ambulocetus* are similar in morphology, bearing a high and connate para- and metacone, and a protocone that is on a broad and low lingual shelf, unlike remingtonocetids where this shelf is narrow. The protocone of *Ambulocetus* is weaker than that of *Pakicetus* (*1*) and *Ichthyolestes* [R. Dehm and T. zu Oettingen-Spielberg, *Bayer. Akad. Wiss. Math. Naturwiss. Kl. Abh.* **91**, 1 (1958)], while the cusp is absent in *Protocetus*. This cusp is well set off from the labial cusps, unlike *Indocetus*. Crests are poorly developed on the teeth of *Ambulocetus*, as in their mesonychid ancestors [F. S. Szalay, *Evolution* **23**, 703 (1969)]. The lower canine is large and single rooted, whereas the four lower premolars have two roots, unlike remingtonocetids. P/4 consists of a single high cusp, unlike *Pakicetus*. The trigonid of M/2 and M/3 is much higher than the talonid, unlike *Gandakasia* and *Pappocetus* (*15*). It lacks a metaconid, unlike *Pakicetus*. *Ambulocetus* lacks the tubercles that occur rostral to the protoconid of *Pappocetus*. Few details of the talonid remain, but there seems to have been a single cusp and no basin, as in *Pakicetus*. Unlike most other archaeocetes, the pterygoid processes are enormous and their dorsoventral extent matches that of the braincase. *Etymology.* The genus name is a combination of ambulare (to walk) and cetus (whale), in recognition of a characteristic mode of locomotion in this cetacean. The species indication, natans (swimming), describes another aspect of its locomotor repertoire.
4. J. G. M. Thewissen, *Natl. Geogr. Res. Expl.* **9**, 125 (1993). Figure 12 shows the type locality for *Ambulocetus natans*. Its caption is wrong.
5. L. Van Valen, *Bull. Am. Mus. Nat. Hist.* **132**, 1 (1966).
6. A. Wyss, *Nature* **347**, 428 (1990).
7. D. A. Pabst, *J Zool.* **230**, 159 (1993).
8. E. J Slijper, *Capita Zool.* (*The Hague*) **6–7**, 1 (1936).
9. *Pachyaena* has 15 caudal vertebrae (*22*), *Basilosaurus* has 21 (*16*), ziphiids have 19, and physeterids have 24.
10. W. D. Matthew and W Granger, *Bull. Am. Mus. Nat. Hist.* **23**, 1 (1915).
11. F. E. Fish, *Mammal Rev.* **21**, 181 (1991).
12. D. P. Aleshire, *J. Vertebr Paleontol. Suppl* **13**, 24A (1993).
13. F. J. Tarasoff, A. Bisaillon, J. Pierard, A. P. Whitt, *Can. J. Zool.* **50**, 915 (1972).
14. A. W. English, *J. Zool.* **178**, 341 (1976).
15. M. P. Beentjes, *Zool. J. Linn. Soc.* **98**, 307 (1990).
16. C. W. Andrews, *Proc Zool. Soc. London* **1919**, 309 (1919).
17. R. Kellogg, *Carnegie Inst. Washington. Publ.* **482**, 1 (1936).
18. R. C. Hulbert Jr. and R. M. Petkewich, *J. Vertebr. Paleontol. Suppl.* **11**, 36A (1991).
19. R. C. Hulbert Jr., *ibid.* **13**, 42A (1993).
20. K. Kumar and A. Sahni, *J. Vertebr. Paleontol.* **6**, 326 (1986).
21. P. D. Gingerich, S. M. Raza, M. Arif, M. Anwar, X. Zhou, *Contrib. Mus. Paleontol. Univ. Mich.* **28**, 393 (1993).
22. P. D. Gingerich, N. A. Wells, D. E. Russell, S. M. I. Shah, *Science* **220**, 403 (1983).
23. X. Zhou, W. J. Sanders, P. D. Gingerich, *Contrib. Mus. Paleontol. Univ. Mich.* **28**, 289 (1992).
24. F. E. Fish, *J. Mammal.* **74**, 275 (1993).
25. ______, in *Mammalian Energetics: Interdisciplinary Views of Metabolism and Reproduction*, T. E. Tomasi and T. H. Horton, Eds. (Cornell Univ. Press, Ithaca, NY, 1992), chap. 3.
26. A. B. Howell, *Aquatic Mammals* (Thomas, Springfield, IL, 1930).

27. We thank A. Aslan, D. P. Domning, F. E. Fish, R. E. Fordyce, P. D. Gingerich, R. C. Hulbert, S. I. Madar, S. M. Raza, K. D. Rose, A. R. Wyss, and the Geological Survey of Pakistan. Field work was supported by the National Geographic Society.

28 October 1993; accepted 3 December 1993

An Inverted Double Seismic Zone in Chile: Evidence of Phase Transformation in the Subducted Slab

Diana Comte and Gerardo Suárez

Data from two microseismic field experiments in northern Chile revealed an elongated cluster of earthquakes in the subducted Nazca plate at a depth of about 100 kilometers in which down-dip tensional events were consistently shallower than a family of compressional earthquakes. This double seismic zone shows a distribution of stresses of opposite polarity relative to that observed in other double seismic zones in the world. The distribution of stresses in northern Chile supports the notion that at depths of between 90 to 150 kilometers, the basalt to eclogite transformation of the subducting oceanic crust induces tensional deformation in the upper part of the subducted slab and compressional deformation in the underlying mantle.

Since the advent of plate tectonics, intermediate and deep earthquakes have been interpreted as evidence of cold lithosphere penetrating into the mantle. At intermediate depths, most subducted lithospheres exhibit down-dip tensional faulting, which has been generally interpreted as resulting from the gravitational pull of the slab (*1–6*). The presence of a more complex state of stress in the subducted slab was observed first in Tohoku, Japan (*7*). There, a sheet of compressional earthquakes lies above a sheet of down-dip tensional events. These two seismic planes are separated by ~40 km at a depth of ~60 km, and they merge at a depth of 200 km. Similar double-planed seismic zones have subsequently been reported in other subduction zones (*7, 8*).

In general, double seismic zones have been associated with the unbending of a subducted slab that undergoes a sharp change in radius of curvature beneath the interplate contact and then becomes straight (*9–11*). All subduction zones, however, suffer this bending, and not all of them exhibit this type of seismicity. Thus, other mechanisms have been proposed (*12*). In this report, we describe a double seismic zone in the subducted Nazca plate beneath the active volcanic arc in northern Chile. The observed distribution of seismicity is inverted relative to other double seismic zones reported in the western Pacific. Thus, the arguments offered to explain the presence of traditional double seismic zones do not account for the inverted polarity of the two bands of seismicity in Chile.

Northern Chile is one of the more active seismic zones of the circum-Pacific belt. The Nazca plate subducts beneath the South American plate with a relative rate of convergence of about 8.4 cm/year (*13*). The last great earthquake occurred there on 10 May 1877 (moment magnitude M_w ~8.7) (*14*). Two local microearthquake investigations were carried out in this seismic gap (*15, 16*). The first experiment was located in the southern end of the 1877 rupture zone, near Antofagasta. A second investigation took place near Iquique, in the middle of the 1877 fault break (Fig. 1). A subset of about 200 microearthquakes were selected from each experiment. We used these earthquakes for the simultaneous two-dimensional inversion of both the hypocenters and the velocity structure in the studied area (*16*).

The observed seismicity is mainly concentrated inland within the downgoing slab. In both experiments, an elongated cluster of earthquakes was located at a depth of ~100 km. In general, fault plane solutions could be determined for the largest and best recorded earthquakes. The focal mechanisms of these events show both normal and reverse faulting in a close spatial relationship, where the down-dip tensional events are consistently shallower than the compressional microearthquakes (Figs. 1 and 2), without showing strong differences in their coda-duration magnitudes (M_d ~3.4 ± 0.3).

For the Iquique survey, the tensional events ranged in depth from 88 to 109 km, and the compressional events had depths varying from 107 to 126 km. In Antofagasta, the tensional events ranged from 81 to 108 km, predominantly with depths of less than 104 km. The compressional events were located between 104 and 122 km in depth. Thus, the change from the tensional earthquakes to the deeper compressional stress field occurs in both regions at a depth of ~105 km. The average separation between the two stress sheets is ~15 km (Fig. 2).

Average hypocentral errors are ±2 km, as obtained from the a posteriori covariance matrix resulting from the joint inversion of hypocenters and the two-dimensional velocity structure (*16*). Besides these statistical errors, we studied the changes of the epicentral coordinates and of the focal depths when modifications were made in the location scheme (for example, a different initial trial depth, changes in Poisson's ratio, and modifications of the velocity structure). During these tests, the hypocentral locations did not change by more than 7 km in a few extreme cases, and in general, the changes were less than 3 to 4 km. Accurate location of the hypocenters was possible because excellent *S* wave readings were available from the three-component digital stations at distances that are smaller than the focal depth of the earthquakes studied.

The change in polarity of the *P* waves is evident in the traces recorded by two seismic stations of a pair of events located at almost the same epicenter but with different focal depths (Fig. 3): event A7 at a depth of 102 km and A10 at a depth of 110 km (Figs. 1 and 2B). Both events were recorded at the same digital stations (SRA and MAR) and share similar azimuth and take-off angles.

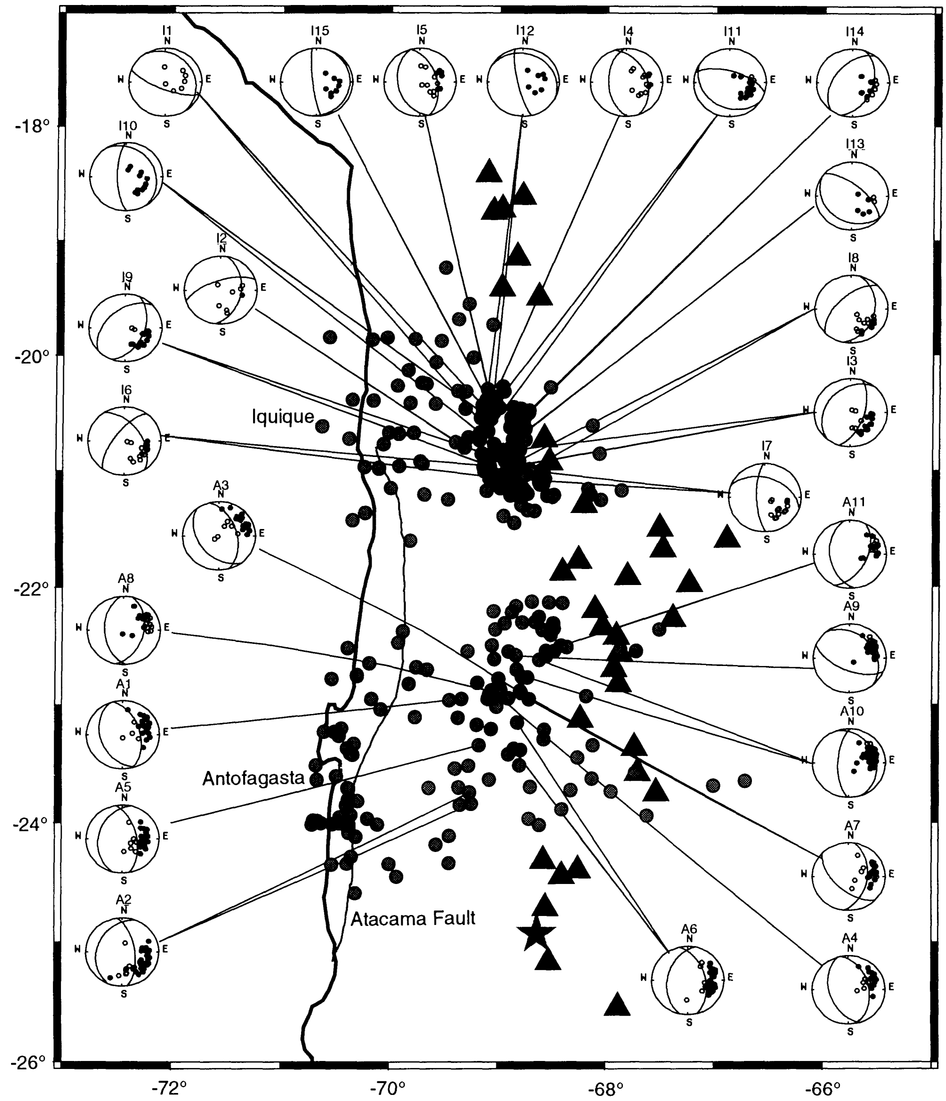

Fig. 1. Epicentral distribution of seismicity recorded by the local seismic networks near Iquique and Antofagasta, northern Chile (solid circles). Lower hemispheric projection of the focal mechanisms show dilations as open circles and compressions as black circles. Triangles represent quaternary volcanoes in the region. The star marks the compressional earthquake of 17 January 1977 (body wave magnitude m_b = 6.0) (*20*).

D Comte, Instituto de Geofísica, Universidad Nacional Autónoma de México, Apartado Postal 70-172, México D.F., 04510 México, and Departamento de Geofísica, Universidad de Chile, Casilla 2777, Santiago, Chile.
G. Suárez, Instituto de Geofísica, Universidad Nacional Autónoma de México, Apartado Postal 70-172, México D.F., 04510 México

In general, the spatial orientation of the auxiliary nodal plane of the individual focal mechanisms is not well constrained. Therefore, and to make sure that we were indeed observing two different families of focal mechanisms, we performed a formal inversion of the best fitting stress tensor based on the first motion polarities of the P waves for each of the two seismic bands (*17*). The focal mechanism solutions (Fig. 1) and the stress tensor (Fig. 4) correspond to those obtained from the inversion. In the case of the deeper tensional earthquakes, the resulting *T* axis of the stress tensor (axis of least compressional stress) is almost horizontal and oriented in an east-west direction. For the compressional earthquakes beneath, the *P* axis (axis of greatest compressional stress) is horizontal and also oriented east-west (Fig. 4). The error estimates determined from the inversion show that the principal axes are within a cone of uncertainty of ~30°.

Intermediate-depth seismicity routinely reported teleseismically in northern Chile is characterized by tensional events (*18*, *19*). However, an intermediate-depth earthquake with a compressional mechanism occurred in northern Chile beneath the Andean volcanic arc (Fig. 1) at a focal depth of 130 km, as determined from a body waveform inversion (*20*). This focal depth clearly places it beneath the sheet of tensional events, which lies at an average depth of 110 km. Kono *et al.* (*21*) also identified this earthquake and suggested the presence of a double seismic zone. However, they incorrectly assumed that the sheet of down-dip tensional events was beneath this reverse-faulting earthquake, as in other subduction zones of the western Pacific. This event suggested the presence of a double-planed seismic zone with the same polarity of stresses as that observed with our local data (*19*) and indicates that the presence of down-dip compressional events beneath a family of tensional earthquakes occurs elsewhere in northern Chile and is not a phenomenon restricted to the Antofagasta and Iquique areas studied here.

Traditional hypotheses offered to explain the presence of double-planed seismic zones (*12*) do not account for our observations because the polarity of the stress sheets predicted by these models is opposite to what is observed in northern Chile. Therefore, the inverted double seismic zone observed in Antofagasta and Iquique is probably associated with a phenomenon different from those usually used to explain the other double seismic zones, which are identified mainly in the western Pacific.

The double seismic zone in northern Chile may be explained by the bending of the slab beneath the volcanic arc. However, the cross sections clearly show no down-

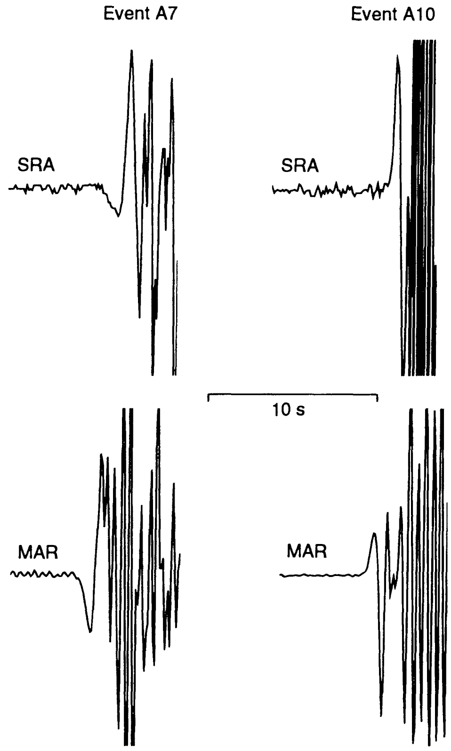

Fig. 3. Seismograms recorded at the digital stations SRA and MAR of events A7 and A10. Note the change of the *P* wave first motion polarity: dilation for the shallower tensional event (A7) and compression for the deeper compressional earthquake (A10). The take-off angles of these stations are near the center of the lower hemispheric projection.

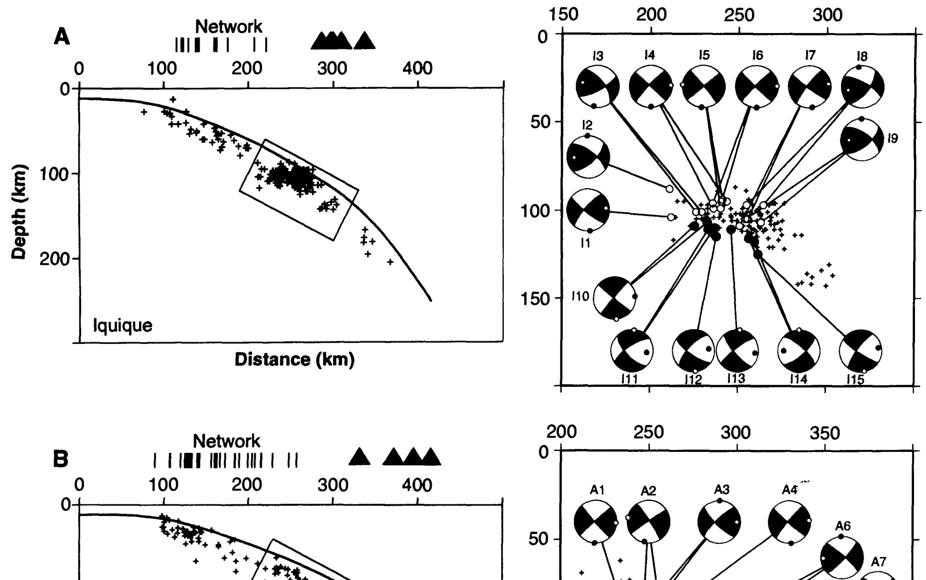

Fig. 2. Cross sections in the direction of convergence of selected events determined for (**A**) the Iquique experiment and (**B**) Antofagasta. The projections of the seismic stations are shown as vertical bars, and triangles correspond to the projections of active volcanoes in the region. The events included in the box are enlarged to the right, where open circles denote the tensional events and solid circles correspond to compressional events. The side-looking, hemispheric projection of the focal mechanism of these events is shown; the axes of greatest (*P* axis) and least (*T* axis) compressional stress are represented by small, black and white dots, respectively. The events are numbered as on Fig. 1.

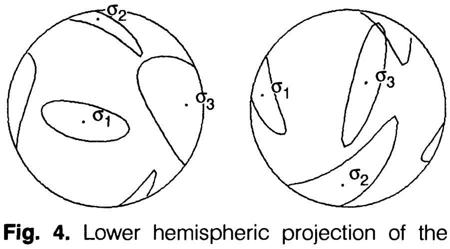

Fig. 4. Lower hemispheric projection of the stress tensors resulting from the inversion for the sheet of tensional events and of compressional earthquakes. Curves around the principal axes of stress are the estimated errors. σ_1 is the *P* axis, σ_3 is the *T* axis, and σ_2 is the *B* axis (intermediate stress).

ward curving of the slab (Fig. 2). On the other hand, the double-planed seismicity in northern Chile is observed beneath the volcanic Andean belt, suggesting it is associated with the generation of magma and the production of arc volcanoes. Thus, it could be explained as a result of a phase change in the slab, as was recently suggested for the Tonga subduction zone (*22*).

Kirby and Hacker (*23, 24*) modeled the distribution of stresses induced by changes in pressure and temperature in the subducting lithosphere at depths of between 90 to 150 km. They argued that oceanic plates have a laminated structure with a thin crust on the top composed of basaltic minerals, overlying a thicker mantle composed mainly of peridotite. According to their numerical results (*25*), the subducting basaltic crust transforms into the denser eclogite as a result of the increased pressure induced during the plate descent and the dehydration of the oceanic crust at the source of the volcanic arc. However, the peridotite composing the upper mantle does not suffer a phase change because it is stable to greater pressure.

This differential volume change produces tensional deformation in the transformed crustal layer and induces a smaller compressional deformation near the top of the underlying mantle (*23, 24*). The distribution of stresses induced by this phase change would explain the inverted double seismic zone observed in northern Chile and the fact that it is observed mainly with events of smaller magnitude. Furthermore, the separation between the stress sheets suggested by the numerical results is similar to that observed in both Iquique and Antofagasta (~15 km).

REFERENCES AND NOTES

1. B. Isacks and P. Molnar, *Nature* **223**, 1121 (1969).
2. ———, *Rev. Geophys.* **9**, 103 (1971).
3. D. Forsyth and S. Uyeda, *Geophys. J. R. Astron. Soc.* **43**, 163 (1975).
4. N. Vlaar and M. Wortel, *Tectonophysics* **32**, 331 (1976).
5. M. Vassiliou, B. Hager, A. Raefsky, *J. Geodyn.* **1**, 11 (1984).
6. W. Spence, *Rev. Geophys.* **25**, 55 (1987).
7. Double seismic zones have been reported beneath Tohoku, Japan, by N. Umino and A. Hasegawa [*Seismol. Soc. Jpn. J.* **28**, 125 (1975)], A. Hasegawa *et al.* [*Tectonophysics* **47**, 43 (1978)], and T. Yoshii [*ibid.* **55**, 349 (1979)]; in the Tohoku-Hokkaido region, Japan, by N. Umino *et al.* [*Seismol. Soc. Jpn. J.* **37**, 523 (1984)]; in Hokkaido, Japan, by S. Suzuki *et al.* [*Tectonophysics* **96**, 59 (1983)]; in Kurile-Kamchatka by W. Stauder and L. Mualchin [*J. Geophys. Res.* **81**, 297 (1976)]; and in the eastern Aleutians by M. Reyners and K. Coles [*ibid.* **87**, 356 (1982)] and L. House and K. Jacob [*ibid.* **88**, 9347 (1983)]. H. Kawakatsu (*11*) gives a thorough review of these and other regions where double seismic zones have been identified.
8. K. Fujita and H. Kanamori, *Geophys. J. R. Astron. Soc.* **66**, 131 (1981).
9. E. R. Engdahl and C. H. Scholtz, *Geophys. Res. Lett.* **4**, 473 (1977).
10. B. Isacks and M. Barazangi, in *Island Arcs, Deep-Sea Trenches, and Back-Arc Basins*, M. Talwani and W. Pitman III, Eds. (Maurice Ewing Ser. 1, American Geophysical Union, Washington, DC, 1977), pp. 99–114.
11. H. Kawakatsu, *J. Geophys. Res.* **91**, 4811 (1986).
12. Proposed mechanisms to explain double seismic zones include stresses associated with phase changes [K. Veith, thesis, Southern Methodist University (1974)], elastic unbending of the slabs (*9, 11*), sagging of the subducted slab under its own weight [T. Yoshii, *Kagaku* **47**, 170 (1977), N. H. Sleep, *J. Geophys. Res.* **84**, 4565 (1979)], and thermo-elastic stresses [K. Goto *et al.*, *Tectonophysics* **112**, 111 (1985); L. S. House and K. H. Jacob, *Nature* **295**, 587 (1982)]. Also, Spence (*6*) suggested that the tensional earthquakes reflect slab pull forces, whereas the shallower compressional earthquakes reflect local resistance to rapid down-dip plate motion.
13. C. DeMets, R. G. Argus, S. Stein, *Geophys. J. Int.* **101**, 425 (1990).
14. D. Comte and M. Pardo, *Nat. Hazards* **4**, 23 (1991).
15. D. Comte *et al.*, *Geophys. J. Int.*, in press.
16. D. Comte, S. Roecker, G. Suárez, *ibid.*, in press.
17. L. Rivera and A. Cisternas, *Bull. Seismol. Soc. Am.* **80**, 600 (1990).
18. L. Astiz, T. Lay, H. Kanamori, *Phys. Earth Planet. Inter.* **53**, 80 (1988).
19. M. Araujo and G. Suárez, *Geophys. J. Int.*, in press.
20. D. Comte and G. Suárez, in preparation.
21. M. Kono, Y. Takahasho, Y. Fukao, *Tectonophysics* **112**, 211 (1985).
22. D. Wiens, J. McGuire, P. Shore, *Nature* **364**, 790 (1993).
23. S. Kirby and B. Hacker, *Eos* **76**, 70 (1993).
24. ———, *ibid.* **72**, 481 (1991).
25. R. Delinger and S. Kirby, *ibid.*, p. 481.

26. We thank C. Mendoza, W. Spence, and two anonymous reviewers for comments that greatly improved this paper. Institut Français de Recherche Scientifique pour le Développement en Coopération (ORSTOM), France, and the International Development Research Centre (IDRC), Canada, offered financial support to conduct the microearthquake investigations. This work was partially funded by Fundación Andes, Chile, grant C-52040. This work was completed while G.S. was visiting the U.S. Geological Survey in Golden, CO.

27 July 1993; accepted 29 October 1993

Modes of Tilting During Extensional Core Complex Development

Drew S. Coleman and J. Douglas Walker

Crustal extension and formation of the Mineral Mountains core complex, Utah, involved tilting of the Mineral Mountains batholith and associated faults during hanging wall and footwall deformation. The batholith was folded in the hanging wall of the Beaver Valley fault between 11 and 9 million years ago yielding about 45° of tilt. Subsequently, the batholith was unroofed along the Cave Canyon detachment fault, and the batholith and fault were tilted approximately 40° during footwall uplift. Recognition of deformed dikes beneath the detachment fault establishes the importance of footwall tilt during formation of extensional core complexes and demonstrates that footwall rebound can be an important process during extension.

Extensional deformation thins the continental crust and results in uplift, cooling, and exposure of ductilely deformed deeper crustal rocks at the Earth's surface in regions known as metamorphic core complexes (*1*). Various models for the development of core complexes and ductile low-angle faults associated with them have been proposed. Models in which extension occurs on an initially steeply or moderately dipping fault that is tilted to low angles through subvertical simple-shear or flexural rotation of the footwall require some tilting to be synchronous with uplift and cooling (*2*). If extension occurs on a low-angle fault, no tilt associated with cooling is predicted (*3, 4*). Many core complexes are comprised dominantly of young batholiths, leading some workers to suggest that cooling and ductile deformation are directly related to intrusion of magmas (*4*). Because batholiths are readily datable, the timing of intrusion, cooling, and faulting can be well established. However, batholiths generally lack planar markers used to determine the structure of core complexes, and thus evaluation of tilting can be difficult. In this report we present data for a dike swarm in the Mineral Mountains batholith that establish the absolute timing of intrusion and deformation in the region and allow estimation of tilting during extension.

The Mineral Mountains (Fig. 1) lie along the southern projection of the Sevier Desert detachment fault (*5, 6*) and are composed dominantly of the 25- to 17-million-year-old granitic Mineral Mountains batholith (*7–14*). The batholith and its wall rocks make up an extensional core complex (*15*), lying in the footwall of the Cave Canyon detachment fault (*10, 12, 16*) and the hanging wall of the listric Beaver Valley fault (*5, 7*). However, the relative timing of motion on these faults has not been clear. Price and Bartley (*15*) suggested that the Cave Canyon detachment fault was initially moderately dipping

D. S. Coleman, Massachusetts Institute of Technology, Department of Earth Atmospheric and Planetary Sciences, 54-1126, Cambridge, MA 02139.
J. D. Walker, Department of Geology, 120 Lindley Hall, University of Kansas, Lawrence, KS 66044.